

# Numerical Prediction of Blood Damage in the Clearance Region for a BiVentricular Assist Device (BVAD) BVAD 틸새 부분에 대한 혈액 손실의 수치적 예측

D. C. Sin, Tan A., H. E. Jeong, B. K. Choi and W. C. Kim  
신동춘 · 앤디 탄 · 정한얼 · 최병근 · 김원철

**Key Words** : Centrifugal blood pump(원심 혈액 펌프), Computational fluid dynamics(CFD), Leakage flow (누출량), BiVentricular Assist Device(BVAD), Thrombosis(혈전증)

**요약** : 전자기적으로 지지되는 임펠러를 가진 원심 혈액 펌프는 기존의 심장 펌프에 비해 많은 장점을 가지고 있지만, BVAD의 틸새에서 발생하는 유체 동역학적인 문제는 여전히 규명이 되지 않은 상태이다. 본 연구에서는 BVAD의 틸새에서 발생하는 혈액외상(blood trauma)의 예측에 대한 연구에 중점을 두고 있다. 일반적으로 원심 혈액 펌프의 설계를 위해 전자기적으로 지지되는 원심 혈액 펌프의 디스크 틸새에서 발생하는 혈액의 손상을 평가하는 방법으로 CFD를 이용한 방법이 널리 이용되고 있다. 따라서, 본 연구에서는 초기 원심 혈액 펌프의 설계 단계에서 펌프의 특성을 평가하기 위하여, 축 방향 틸새의 영향과 회전수 변화에 따른 누수경로의 전단 응력의 크기 평가를 CFD를 사용하여 해석하여 보았다.

## 1. Introduction

Implantable VADs using centrifugal blood pumps are being developed and are seeing clinical use in many institutions<sup>1)</sup>.

However, an implantable BVAD is uncommon; hence, the current research focuses on the development of a BVAD for long term implantation. Many studies on the flow pattern within the pump were carried out to predict the influence of blade geometry on hemolysis and thrombus formation<sup>2)</sup>.

However, flow stagnation within the gap region between the rotating impeller hub and casing may lead to thrombus formation.

The clearances, therefore, should be optimised to produce enough leakage flow to achieve the lowest thrombosis and the highest possible pump efficiency.

The flow behaviour in the narrow clearance can be investigated experimentally but only in a limited area and constructing the entire flow field requires a great deal of time, although the results are fairly reliable<sup>3)</sup>.

Indeed, measurements of radial and axial velocity components are very difficult for a clearance size of less than 1 mm<sup>2)</sup>.

Computational fluid dynamics (CFD) is adopted in this article as it provides an effective method to predict blood damage in the clearance region of the BVAD at different axial clearance and rotational speeds.

## 2. Materials and Method

### 2.1 Initial BVAD design

Fig. 1 shows the three-dimensional computer assisted design (3D-CAD) model of the pump. The rotary BVAD design includes a left and right

접수일 : 2007년 4월 13일, 채택확정 : 2007년 5월 29일

김원철(책임저자): 경상대학교 기계항공공학부,

해양 산업 연구소

E-mail : wckim@gaechuk.gsnu.ac.kr Tel:(055)640-3122

신동춘, Tan Andy: Institute of Health and Biomedical  
Innovation Queensland University of  
Technology

정한얼: 국립 경상대학교 대학원 정밀기계공학과

최병근: 경상대학교 기계항공공학부, 해양 산업 연구소

impeller positioned on a common rotating hub to form a double sided magnetically and hydrodynamically suspended centrifugal impeller.

The vanes of each side are designed to produce the pressure differential and perfusion rates required of the systemic and pulmonary systems.<sup>4)</sup>

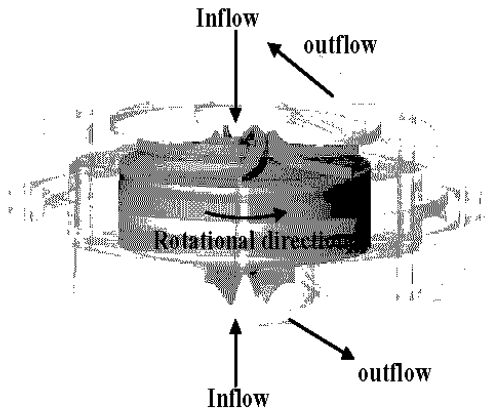


Fig. 1 3D-CAD of the BVAD

The impeller can be moved by magnetic force toward LVAD or RVAD. This movement enabled the single BVAD device to output varying flow rates from the left and right outlets in response to the requirements of the systemic and pulmonary circulatory systems.<sup>5)</sup> In this study, the radial clearance initially between pump hub and casing was set at  $0.25\text{ mm}$  and the axial clearance of LVAD and RVAD when the impeller is situated in the axially neutral position is  $0.5\text{ mm}$ .

## 2.2 Pump performance

Previous experimental measurements<sup>6)</sup> were used to support the CFD predictions on leakage flow rate. The LVAD and RVAD performance tests were conducted using the impeller centrally located within the dual pump cavity. The impeller was mounted on a conventional shaft and sealed bearings, and its axial displacement was changed using a micrometer mechanism in order to simultaneously alter the clearances above the left and right semi-open impeller blades. The

performance test demonstrated that the pump is sensitive to the axial clearance to provide variable flow rates and pressure. The pump operating point of  $5.1\text{ l/min}$  and  $2,200\text{ rpm}$  considered in the effect of the pump position study it represents the average flow rate for each cardiac cycle in this pump.<sup>7)</sup>

## 3. CFD Analysis

### 3.1 Mathematical model

This preliminary study attempts to model leakage flow in the clearance between the rotating hub and stationary housing. Leakage flow is due to high pressure fluid leaving the impeller trailing edge of LVAD impeller and flowing to the trailing edge of RVAD impeller via the clearance between the rotating impeller and stationary housing. With centrifugal blood pumps, the impeller design has been less important than the design of the impeller suspension system for avoiding thrombus formation<sup>8)</sup>. The simplified cylindrical model contains rotating wall with angular velocity  $\omega$ , and a stationary wall; the walls have an inner radius,  $R_1$ , of  $22.5\text{ mm}$  and an outer radius,  $R_2$ , of  $50\text{ mm}$ .

The CFD model itself was generated using GAMBIT (Version 2.2.30, Fluent, Inc), a pre-processor. The cell type for the gaps in the model is a hexahedron, and the number of element was approximately 320000. FLUENT (Version 6.2.16, Fluent, Inc), a proprietary CFD package, was utilised for the processing and post-processing of the model.

The flow is modelled as an incompressible fluid because the density of blood is constant. Although it is known that blood is non-Newtonian fluid, blood viscosity is almost constant under conditions of shear rate above  $100\text{ S}^{-1}$ . The properties assumed for the working fluid were a viscosity of  $0.0036\text{ Pas}$  and a density of  $1059\text{ kg/m}^3$ , which are comparable with those of blood.<sup>9)</sup>

The flow through the pump was assumed to be

steady state<sup>9)</sup>. No-slip conditions were also assumed for all the walls contacting the fluid. Blood flow is modelled by the momentum and mass conservation equations for an incompressible fluid. The  $k-\epsilon$  turbulence model was used in these calculations.

In conclusion, the blood flow in the clearance gap is incompressible, steady state, turbulent flow with a Newtonian liquid. The corresponding steady state ( $\partial/\partial t=0$ ) governing equations in vector notation for incompressible flow with constant viscosity are:

$$\rho(V \cdot \nabla)V = -\nabla p + \rho g + \nabla \cdot \sigma \quad (1)$$

$$\nabla \times V = 0 \quad (2)$$

with  $\rho$  corresponding to the mass density,  $V$  representing the velocity of the fluid,  $P$  as the pressure,  $g$  denoting the body forces,  $\sigma$  signifying the stress tensor.

The maximum Reynolds Number in the clearance area was found to be 863.9 at 2200 rpm, this was below 1500, which is the limiting Reynolds Number for this situation, so the flow was thus assumed to be laminar<sup>10 12)</sup>. Two control parameters for these computations are the rotational speed and the pressure at the inlet boundary. A wide range of operating conditions has been studied: rotational speed varied from 1800 to 2700 rpm, while the pressure difference varied from 55 to 72  $mmHg$ .

### 3.2 Calculation of scalar shear stress

The shear stress in blood is comprised of molecule viscosity stress and Reynolds stress components. Molecule viscosity stress derives from the multiplication of viscosity and the mean velocity gradients. The shear stress tensor is described by the following equation.

$$\sigma_{ij} = \tau_{ij} + \eta_{ij} \quad (3)$$

Where  $\tau_{ij}$  and  $\eta_{ij}$  are molecule viscosity stress and Reynolds stress, respectively, which are given as follows:

$$\tau_{ij} = \mu \left( \frac{\partial u_i}{\partial x_j} + \frac{\partial u_j}{\partial x_i} \right) \quad (4)$$

Where  $\mu$  is the fluid dynamic viscosity, and the last term on the right-hand side of Eq. (1) is the Reynolds stress tensor given by:

$$\eta_{ij} = \mu_t \left( \frac{\partial u_i}{\partial x_j} + \frac{\partial u_j}{\partial x_i} \right) - \frac{2}{3} \rho k \delta_{ij} \quad (5)$$

Where  $\mu_t$  is the turbulent viscosity and  $\delta$  is the Kronecker delta.

High rotational speed and small size (the gap between impeller hub and housing) may make hemolysis a potential threat in centrifugal blood pumps. For laminar flow, the Reynolds stress tensor is zero. A scalar stress value can be obtained according to Bludszweit's stress formula:

$$\sigma = \left[ \frac{1}{6} \sum (\sigma_{ii} - \sigma_{jj})^2 + \sum \sigma_{ij}^2 \right]^{\frac{1}{2}} \quad (6)$$

where  $\sigma$  is the scalar stress (pa)

$\sigma_{ij}$  is the stress tensor.

## 4. Results and Discussion

### 4.1 Effect of the pump position

The scalar shear stress is computed on every node and the elements then are classified by magnitude of stress, and the element's masses are summed up for each class (Fig. 2). This allows for a characterization of the general stress load of the blood within the clearance gap<sup>13)</sup>. The mass-weighted average scalar shear stresses for 0.2  $mm$ , 0.5  $mm$ , and 0.8  $mm$  axial clearances are presented in Table 1. Neutral position result, the 0.5  $mm$  clearance data, is used as a basis for comparison. The clearance in the left pump increases and outflow is reduced, thereby decreasing the blood flow to the systemic circulation. This process effectively increases the output for the right side of the heart, while decreasing output for the left side of the heart.

When the clearance was then reduced to 0.2 mm, the mass weighted average scalar shear stress was significantly increased, to approximately 38 % of the neutral position value. On the other hand, actuating the impeller toward the left chamber reduced left impeller axial clearance and thus improved left outflow while simultaneously increasing the right impeller axial clearance and thus reducing right output. This process effectively increases the output for the left side of the heart, while decreasing output for the right side of the heart. In the case of CASE 3, the result shows a small reduction, with about 84 % of the CASE 2.

Table 1 Effect of the pump position on scalar on scalar shear stress

	CASE1	CASE2	CASE3
Pressure difference (mmHg)	55	61	72
Speed (rpm)	2,200	2,200	2,200
Axial Clearance (mm)	0.2	0.5 (Neutral position)	0.8
Mass-Weighted Average Scalar Shear Stress (Pa)	54	39	33

These results indicate that movement of the impeller towards the right chamber can increase blood damage and movement towards the left chamber can reduce blood damage in the clearance gap. Therefore, incensement of mass weighted average scalar shear stress due to movement of the impeller towards the right chamber may cause thrombosis formation.

Maximum scalar stresses of approximately 600 Pa are achieved at CASE 1. The threshold levels of 500 Pa have been reported as the design condition in the development of centrifugal blood pump for exposure times of 0.1 s<sup>13,14</sup>. Therefore, exposing the blood cells to such levels of fluid stress will likely result in blood trauma based on these computational results.

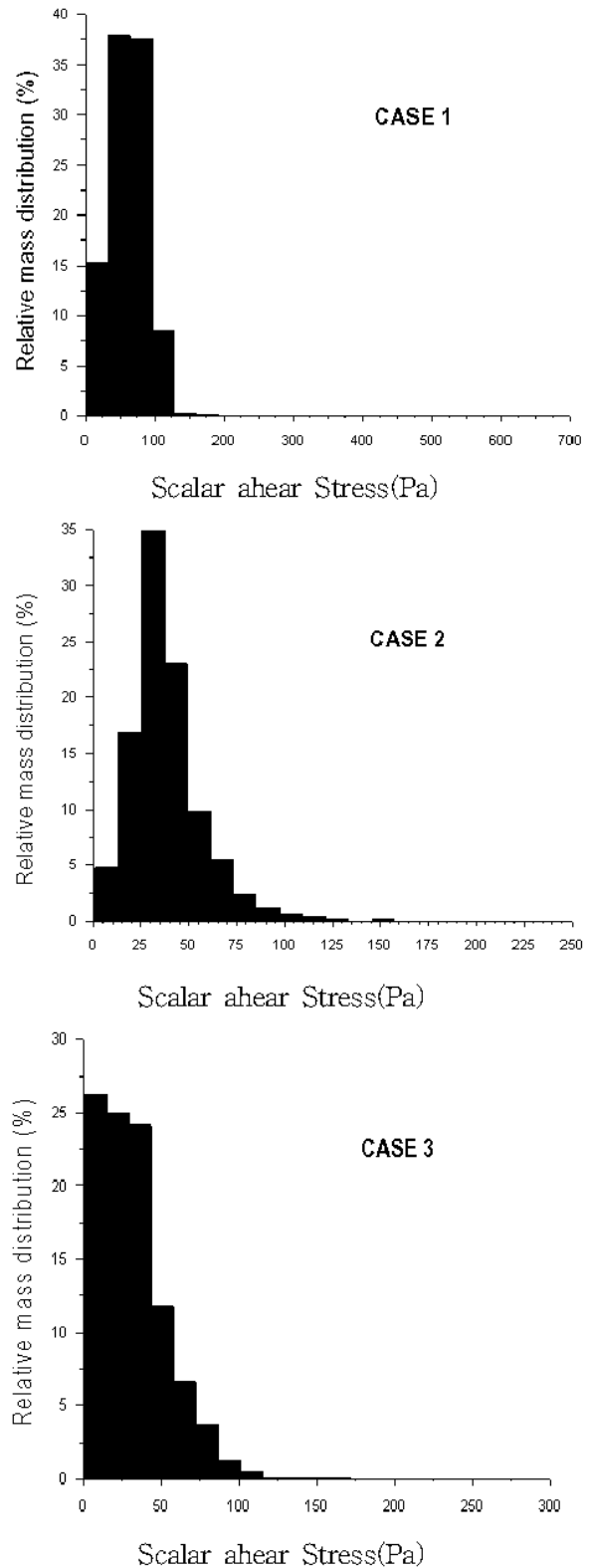


Fig. 2 Mass weighted distribution of scalar shear stress in different axial clearance gap

#### 4.2 Effect of rotational speed

The effect of pump speed on scalar shear stresses was investigated as shown in Table 2. The pump operating conditions selected were a

flow rate of 5.1 L/min and supply pressures of 85 and 24 mmHg for the LVAD and the RVAD, respectively.

Therefore, the boundary condition is a pressure difference 61 mmHg between the volute of the LVAD and the RVAD (Table 2). The relative weighted distribution of scalar shear stresses in the clearance gap under different rotational speed are presented in Fig. 3, from this it is apparent that mass-weighted average scalar shear stresses are in proportion to rotational speed.

To have a low blood damage levels it is essential to have low impeller rotational speed between the fluid and the rotating hub surface. A lower inertia factor is an indication that the pump is more efficient in ensuring a low blood trauma.

Consequently, flow reversal by centrifugal force may be generated in the clearance gap to block blood flow and cause the hemolysis and thrombosis phenomenon.

Table 2 Effect of the pump speed on scalar shear stress

	CASE 4	CASE 5	CASE 6
Pressure difference (mmHg)	61	61	61
Speed (rpm)	1,800	2,200	2,700
Axial Clearance (mm)	0.5	0.5	0.5
Mass-Weighted Average Scalar Shear Stress (Pa)	34	39	48

The lower rotational speed will require less power consumption and should produce lower levels of blood shear. In future studies, the CFD predictions will be compared quantitatively to data that are being obtained using PIV measurements.

It is therefore recommended that the pump should be redesigned to reduce possibility of thrombus event allowing for long term use. The trends of the scalar shear stresses are consistent with earlier published results<sup>15)</sup>, and the agreement provides some validity to the model and assurance to use it for evaluation of new prototype pump designs.

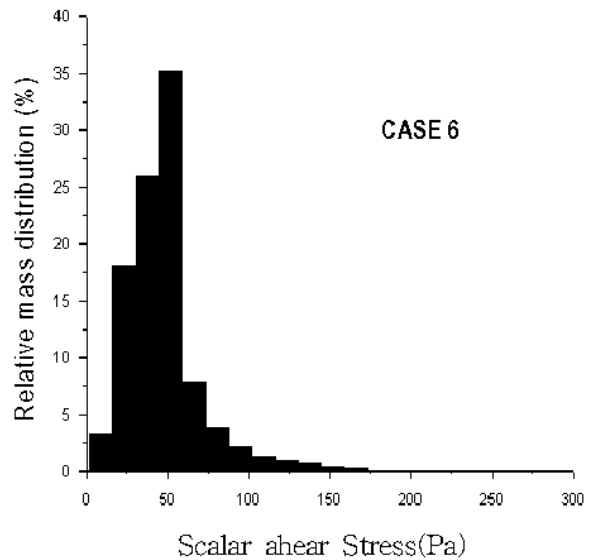
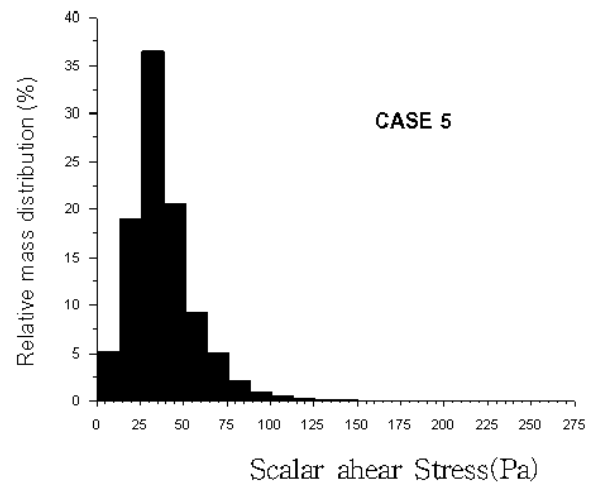
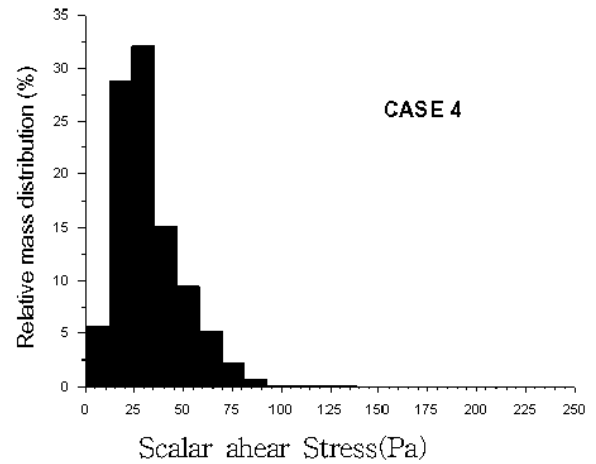


Fig. 3 Mass weighted distribution of scalar shear stress in different impeller speed

### 5. Conclusion

Computational fluid dynamics is a very

important tool that can be used effectively to evaluate and improve pump design. The main focus of this study was to assess the effects of different axial clearance and impeller rotational speed on the scalar shear stress. The present study has shown that the scalar shear stresses are dependent on axial clearance size and rotational speed in the BVAD and that moving the impeller towards the rights chamber may cause thrombosis formation due to high scalar shear stresses.

#### Acknowledgement

This is supported by Second-phase Brain Korea 21 project and New University for Regional Innovation project in 2006 years.

#### References

1. Kojiro Furukawa, T.M., Yukihiko Nose, 2005, "Right Ventricular Failure After Left Ventricular Assist Device Implantation: The Need for an Implantable Right Ventricular Assist Device", *Artificial Organs*, Vol. 29, No 5, pp. 369-377.
2. Chan, W.K., T. Akamatsu, and H.D. Li, 2000, "Analytical Investigation of Leakage Flow in Disk clearance of a Magnetically Suspended Centrifugal Impeller", *Artificial Organs*, Vol. 24, No 9, pp. 734-742.
3. Nishida, M. and T. Yamane, 2004, "Geometric Optimization for Non-Thrombogenicity of a Centrifugal Blood Pump through Computational Fluid Dynamic Analysis", *JSME International Journal*, Vol. 47, No. 4, pp. 1108-1116.
4. Timms, D.L., 2005, "Design, Development and Evaluation of Centrifugal Type Ventricular Assist Devices", in *Engineering Systems. Queensland University of Technology: Brisbane*, p. 300.
5. Timms, D., Design, 2005, "Development and Evaluation of Centrifugal Ventricular Assist Device", in *School of Engineering Systems. Queensland University of Technology: Brisbane*.
6. Daniel Timms, et al., 2006, "Left/Right Flow Balancing With A Rotary Bi-Ventricular Assist Device", *Artificial Organs*, Vol 30, No 11, pp. A44.
7. Daniel Timms, M.H., Andy Tan, and Mark Percy, 2005, "Evaluation of Left Ventricular Assist Device Performance and Hydraulic Force in a Complete Mock Circulation Loop", *Artificial Organs*, Vol. 29, No. 7, pp. 573-580.
8. Tsukiya, T., et al., 2002, "Improvement of Washout Flow in a Centrifugal Blood Pump by a Semi-open Impeller", *ASAIO Journal*, Vol. 48, No. 1, pp. 76-82.
9. Kido, K., et al., 2006, "Computational Fluid Dynamics Analysis of the Pediatric Tiny Centrifugal Blood Pump (TinyPump)", *Artificial Organs*, Vol. 30, No. 5, pp. 392-399.
10. Yamane, T., et al., 1999, "Flow Visualization Measurement for Shear Velocity Distribution in the Impeller-Casing Gap of a Centrifugal Blood Pump", *JSME International Journal*, Vol. 42, No 3, pp. 621-627.
11. Ikeda, T., et al., 1996, "Quantitative visualization study of flow in a scaled-up model of a centrifugal blood pump", *Artificial Organs*, Vol. 20, No 2, pp. 132-138.
12. Chua, L.e.a, 2004, "Leakage Flow Rate and Wall Shear Stress Distributions in a Biocentrifugal Ventricular Assist Device", *ASAIO Journal*, Vol 50, pp.530-536
13. Apel, J., et al., 2001, "Assessment of Hemolysis Related Quantities in a Microaxial Blood Pump by Computational Fluid Dynamics", *Artificial Organs*, Vol. 25, No. 5, pp. 341-347.
14. Paul, R., et al., 2003, "Shear stress related blood damage in laminar couette flow", *Artificial Organs*, Vol. 27, No. 6, pp. 517-529.
15. Chan, W.-K. and -W. Wong, A Review of Leakage Flow in Centrifugal Blood Pumps. *Artificial Organs*, 2006. 30(5): p. 354-359.